

Wear resistant solid lubricant coating made from PTFE and epoxy

N.L. McCook^a, D.L. Burris^a, G.R. Bourne^a, J. Steffens^a, J.R. Hanrahan^b and W.G. Sawyer^{a,*}

^aDepartment of Mechanical Engineering, University of Florida, Gainesville, FL 32611

^bW.L. Gore & Associates, Elkton, MD 21922

Received 5 April 2004; accepted 15 August 2004

A composite coating of polytetrafluoroethylene and epoxy shows 100 × improvements in wear resistance as compared to either of its constituents alone and reduced friction coefficient under testing on a pin-on-disk tribometer. This coating is made by impregnating an expanded PTFE film with epoxy, which provides three unique functions: (1) the epoxy compartmentalizes the PTFE nodes, which is believed to reduce the wear of the PTFE, (2) the epoxy increases the mechanical properties such as elastic modulus and hardness, and (3) the epoxy provides a ready interface to bond the films onto a wide variety of substrates easily and securely. The experimental matrix had normal loads of 1–3 N, sliding speeds from 0.25 to 2.5 m/s, and used a 2.4 mm radius low carbon steel pin in a rotating pin-on-disk tribometer. The skived PTFE films had wear rates on the order of $K = 10^{-3} \text{ mm}^3/\text{Nm}$ and friction coefficients around $\mu = 0.2$. Both the high density films (70 wt% PTFE) and low density films (50 wt% PTFE) had wear rates on the order of $K = 10^{-6} \text{ mm}^3/\text{Nm}$ and friction coefficients around $\mu = 0.15$. The neat epoxy films showed significant scatter in the tribological measurements with wear-rates on the order of $K = 10^{-4} \text{ mm}^3/\text{Nm}$ and friction coefficients around $\mu = 0.40$. The enhanced tribological behavior of these composites is believed to stem from the coatings ability to draw thin PTFE transfer films into the contact from the nodes of PTFE, which act like reservoirs. Nanoindentation mapping of the coatings and the transfer films supports this hypothesis, and accompanies scanning electron microscopy observations of the worn and unworn coatings.

KEY WORDS: solid lubricants, coatings, composites, PTFE

1. Introduction

There is great enthusiasm for wear-resistant, inert, environmentally insensitive, low friction, polymeric tribological coatings. Polytetrafluoroethylene is an exceptional low friction polymeric material that is used in many bearing applications as a solid lubricant. Unfortunately, PTFE suffers from poor wear resistance, and is thus the subject of many tribological research projects in the area of composites [1]. Such research often incorporates hard filler particles into the PTFE matrix such as glass fibers [2], copper [3], ceramics [4], carbon fibers [5], chopped carbon fibers [6] and nano particles [7,8] in an effort to enhance the wear resistance. Other research groups incorporate fillers that may act as additional solid lubricants such as bronze [9,10], graphite [3], carbon nanotubes [11], molybdenum and tungsten disulfide [12], lead [13–15], and boric-oxide [16] to improve wear resistance while retaining low friction coefficients. PTFE is also frequently used as filler in polymeric materials that have good mechanical properties but poor tribological properties, such as polyoxymethylene [17,18], epoxy [19], polyetheretherketone [20], and polyimide [21].

Recently, there have appeared publications looking at the tribological worthiness of nanocomposites made

with epoxies, which in its neat form is a notoriously poor tribological performer. Silica [22], alumina [23], and silicon nitride [24] nano particles have all been incorporated into epoxies with most additions improving both the coefficient of friction and wear resistance. There is also work that has incorporated fluorinated polyaryletherketone into epoxy to create a polymer/epoxy blend that, in the main, shows roughly 20% reductions in friction coefficient [25]. As mentioned above, PTFE has also been used as filler in epoxy matrixes.

This work reports on a new type of solid lubricating PTFE composite that utilizes expanded PTFE films as the scaffolding and epoxy as reinforcement. This composite, which is processed as a thin film, can then be relatively easily bonded to various substrates via the epoxy. Unlike most of the other PTFE composites mentioned, bearing components can be coated with the composite film as opposed to being machined from a compression molded composite billet.

2. Description composite preparation

Expanded PTFE films were prepared for this study. As compared to skived PTFE films (full density) expanded PTFE has a number of unique properties. Most noticeably, the material is porous with nodes of

*To whom correspondence should be addressed.
E-mail: wgsawyer@ufl.edu

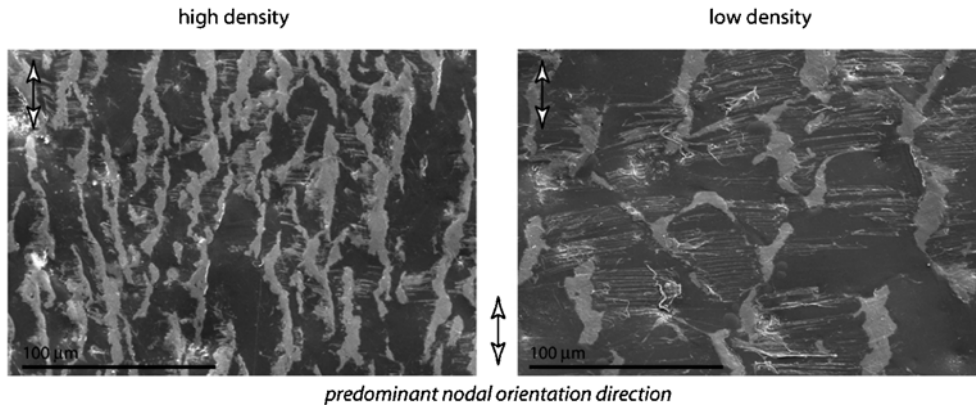


Figure 1. Scanning electron microscopy images of the top view of the PTFE (light gray) and epoxy (dark gray) composites. The predominant nodal direction of the PTFE is indicated by the white open arrowheads.

dense PTFE being connected to other nodes through a network of PTFE fibrils. The expanded PTFE films can have a wide range of engineered node shapes and spacing, with porosities easily ranging from 5 to 90%. Additionally this node and fibril structure of expanded PTFE films provides increased strength to weight ratio and creep resistance as compared to fully dense PTFE films ($\rho = 2200 \text{ g/mm}^3$). Two different expanded PTFE films were created for this study. They were approximately $200 \mu\text{m}$ in thickness with initial densities of $\rho = 400 \text{ g/mm}^3$ (low density) and $\rho = 950 \text{ g/mm}^3$ (high density), which corresponds to a PTFE volume fraction of 0.18 and 0.43, respectively.

The expanded PTFE films were combined with an uncrosslinked epoxy, which resulted in a PTFE weight percent of 70% for the high density film and 50% for the low density film. The films were then cured under pressure onto a carbon steel circular disk that had an average roughness of $R_a = 2.0 \mu\text{m}$. Scanning electron microscopy images of the resulting films are shown in figure 1. The high density composite coating had a PTFE volume fraction of $\forall_{\text{PTFE}} = 0.56$ and was approximately $150 \mu\text{m}$ thick (as measured under a scanning white light interferometer). The resulting low density composite coating had a PTFE volume fraction of $\forall_{\text{PTFE}} = 0.35$ and was approximately $100 \mu\text{m}$ thick. The weight percentages did not change under consolidation and curing, and the films were nearly free of pores.

3. Experimental procedure

Experiments were run on an open rotating pin-on-disk tribometer that is located in a soft-walled clean-room, within a conditioned laboratory environment. The relative humidity varied between 25 and 50% during these tests. The experimental conditions are shown in figure 2. Briefly, the matrix was a 2×2 in sliding speed (0.25 & 2.5 m/s) and normal load (1 & 3 N) with a centerpoint (1 m/s & 2 N) that was repeated

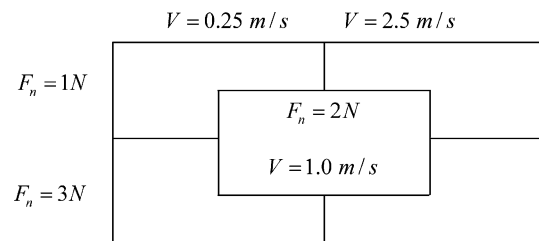


Figure 2. Experimental test matrix (load and speed). The wear track diameters were varied although tests were run the same number of revolutions. Low carbon steel pins with a radius of 2.4 mm were used for all tests.

five times. The pin was a 2.4 mm radius low carbon steel sphere with an initial average roughness of $R_a = 150 \text{ nm}$. The pin was held stationary at the end of the loading arm. A schematic of the experimental apparatus is shown in figure 3. The tribometer uses dead weight loading and records friction forces through a load cell that is located behind a low-friction gimbal. Concentric circular wear tracks are positioned on the disk surface using a micrometer and stage that holds the pin-arm and load cell assembly. Thus, during testing the normal load and sliding speed were prescribed but the wear track diameters and the rotating speed of the disk were varied.

Four different films were evaluated: skived PTFE (fully dense), high density composite, low density composite, and an unfilled epoxy. Because the normal load was controlled during this testing and each coating has a different elastic modulus the initial contact pressures varied from sample to sample. Table 1 provides estimates of the peak contact pressures for each of these films under the three different loads tested. The calculations used a Hertzian contact analysis for all the films, and additionally used an elastic foundation model for the high and low density films, which were significantly thinner than the fully dense PTFE film and the epoxy sample. The maximum subsurface shear stress depth is also indicated in table 1, and in all cases is less than this film thickness.

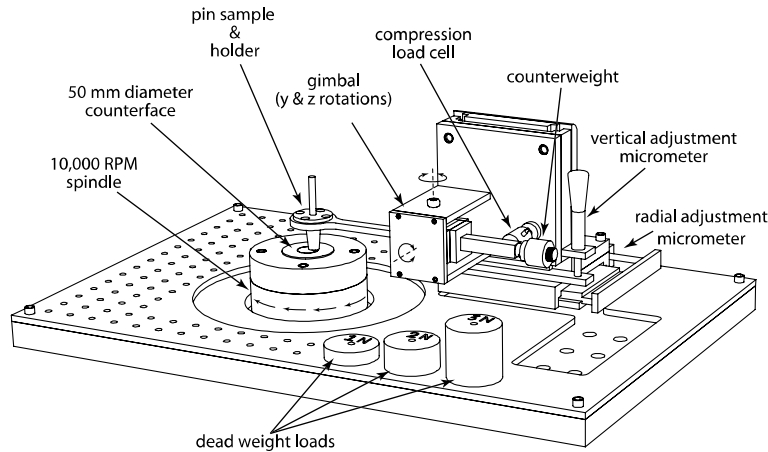


Figure 3. Schematic of the pin-on-disk tribometer.

Table 1.

Initial central contact pressures P calculated using a circular Hertzian contact model (subscript H) or an elastic foundation model (subscript W). The subsurface location of maximum shear stress calculated using the Hertzian contact analysis is given by δ . The elastic properties were determined from indentation testing and the Poisson's ratio was assumed to be $\nu = 0.40$.

	Skived PTFE $E = 1.3 \text{ GPa}$	High density $E = 2.9 \text{ GPa}$	Low density $E = 4.0 \text{ GPa}$	Epoxy $E = 4.6 \text{ GPa}$
$F_n = 1 \text{ N}$	$P_H = 43 \text{ MPa}$ $\delta = 51 \mu\text{m}$	$P_H = 73 \text{ MPa}$ $\delta = 39 \mu\text{m}$	$P_H = 91 \text{ MPa}$ $\delta = 35 \mu\text{m}$	$P_H = 99 \text{ MPa}$ $\delta = 33 \mu\text{m}$
$F_n = 2 \text{ N}$	$P_H = 54 \text{ MPa}$ $\delta = 64 \mu\text{m}$	$P_H = 92 \text{ MPa}$ $\delta = 49 \mu\text{m}$	$P_H = 115 \text{ MPa}$ $\delta = 44 \mu\text{m}$	$P_H = 129 \text{ MPa}$ $\delta = 42 \mu\text{m}$
$F_n = 3 \text{ N}$	$P_H = 62 \text{ MPa}$ $\delta = 73 \mu\text{m}$	$P_H = 105 \text{ MPa}$ $\delta = 56 \mu\text{m}$	$P_H = 131 \text{ MPa}$ $\delta = 50 \mu\text{m}$	$P_H = 148 \text{ MPa}$ $\delta = 48 \mu\text{m}$

Friction coefficient was calculated and recorded during testing through a computer data acquisition system. Each second an average value of the coefficient of friction along the wear track is calculated and recorded. A plot of the coefficient of friction versus time is shown in figure 4 for the four different films evaluated.

Wear tracks were examined post-test under optical microscopy and a scanning white-light interferometer. Wear volumes were calculated by measuring four locations along the wear track and numerically integrating the interferometry data to obtain the cross-sectional area. The average cross-sectional area is then multiplied by the circumference to obtain an estimate of the volume of the wear track. Because the wear track geometry includes both wear and creep damage gravimetric analysis was also used as a check for the volume calculation. A dead weight load of 3 N on the pin sample resting against each film at a stationary location for 8 h: there were no detectable indentations on the films containing epoxy. In the case of the skived PTFE creep was significant and wear rate calculations used gravimetric analysis for this case. However, mass loss measurements were not reliable for the epoxy containing films because of water uptake in the epoxy.

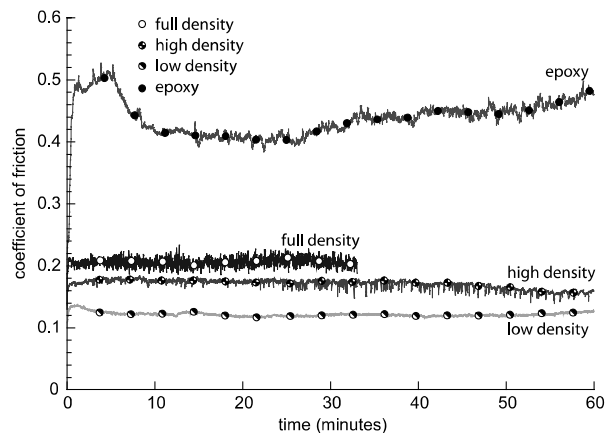


Figure 4. Friction coefficient traces versus time for one experiment under 2 N load and 1 m/s sliding speed. These experiments were repeated five times and the traces shown here represent typical behavior. Legend: full density is a skived PTFE, high density is a 70 wt% PTFE film, low density is a 50 wt% film, and the epoxy contains no PTFE

4. Results and discussion

The experimental results are given in figure 5. The friction coefficients and the wear rates versus weight percent of epoxy are plotted in figure 6. It is readily

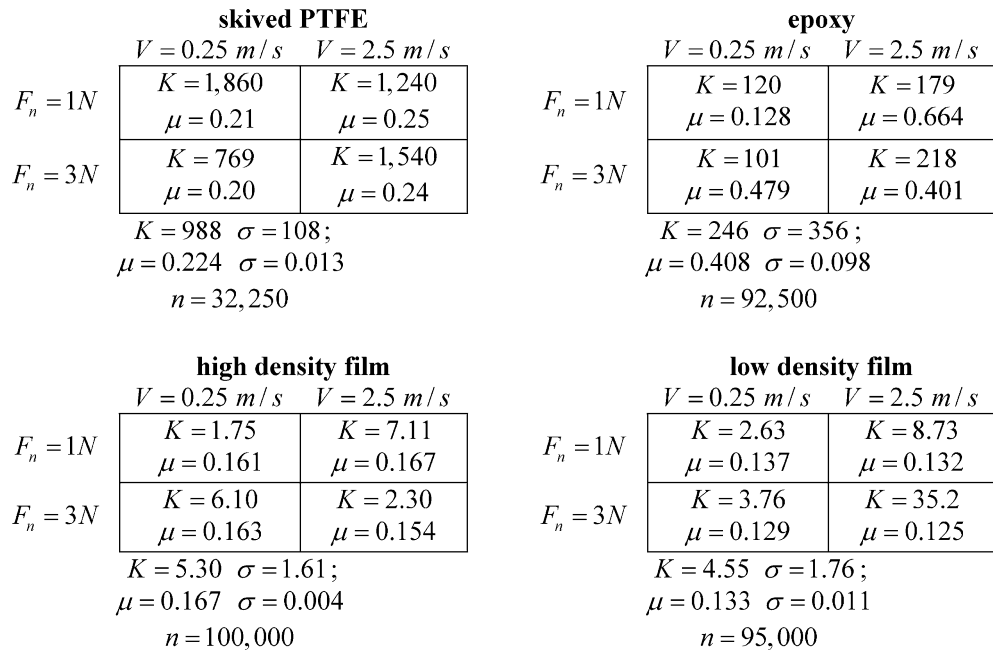


Figure 5. Average wear rate, $K \times 10^{-6} \text{ mm}^3/\text{Nm}$, and friction coefficient, μ , for experiments run under the various matrix conditions. Five repeat experiments under the 2 N load and 1 m/s sliding speed were run on each material. The average values for wear rate and friction coefficient for all repeat experiments along with the standard deviation is given at the bottom of each chart along with the average number of cycles, n , for each experimental series.

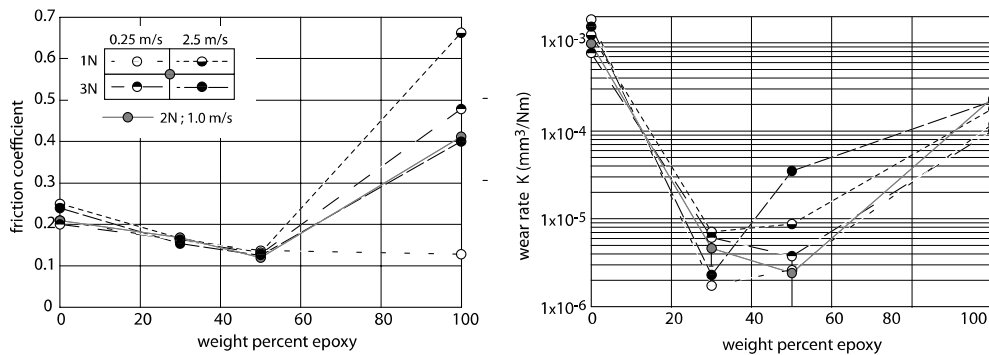


Figure 6. (a) Average friction coefficient versus wt% epoxy, (b) single point measurements of wear rate versus wt% epoxy. The experimental conditions are shown in the inset of the friction coefficient graph. The raw data is given in table 2, the error bars are calculated from the standard deviation of the five repeat experiments at 2 N load and 1.0 m/s sliding speed.

apparent that these films do not operate via a rule-of-mixtures, as both the wear rate and friction coefficient are lower than either of the constituents alone. The origin of the reduced friction is believed to be related to the low shear strength PTFE films being drawn out from nodes into a transfer film that covers the epoxy. Because the elastic modulus of these films is increased by the addition of the epoxy, the contact areas are likely reduced as compared to the full density PTFE.

To examine such a hypothesis scanning electron microscopy of the wear tracks was performed. Scans where the sliding direction is parallel and transverse to the direction of nodal orientation were taken from the same wear track. This is shown in figure 7. The high density film shows PTFE enrichment and the low den-

sity film shows a more complex transfer film that is a mixture of PTFE and epoxy.

Nanomechanical testing was done on both the unworn surfaces and on the transfer films within the wear tracks using a depth sensing indentation technique on a Hysitron Triboindenter. The hardness for such tests is defined as the ratio of the maximum load divided by the project contact area (units of pressure). The depth sensing technique uses a calculated area based on the depth of indentation, where the tip area function was generated by curve fitting a plot of residual projected area versus contact depth from indentations on a fused quartz standard with a manufacturer reported modulus of 72 GPa and Poisson's ratio of 0.070. For this study a Berkovich diamond indenter

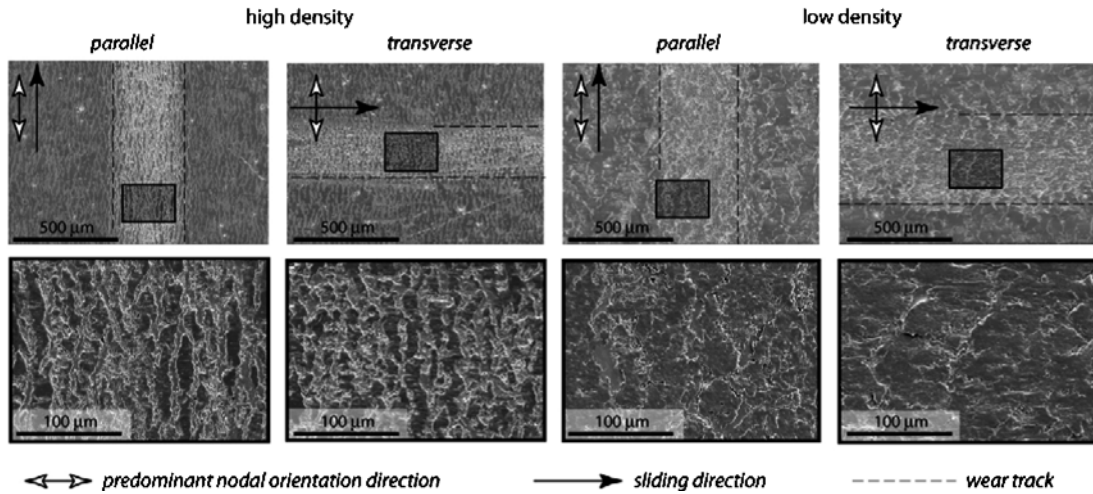


Figure 7. Scanning electron microscopy of films. These experiments were run under 2 N normal load and 1 m/s sliding speed. The upper images show the wear tracks through the film where the sliding direction of the ball over the surface is parallel or transverse to the direction of predominant nodal orientation.

with a total included angle of 142.3°, a half angle of 65.3°, and a tip radius of 100–200 nm was used. Unloading force displacement curves were analyzed to determine reduced modulus and hardness using a method first described by Doerner and Nix [26] and later refined by Oliver and Pharr [27].

Automated indentation over a grid of 25 × 25 points with indentation spacing of 5 μm was run on original surfaces and inside wear tracks. For these experiments a load of 0.5 m N was applied at 0.1 m N/s, held for 5 s, and then unloaded at 0.1 m N/s. For the

skived PTFE and the epoxy samples 30 indents were performed to gather statistics about the parent materials in the composites.

In figure 8, maps of the hardness and modulus (from the same samples as shown in figure 7) are given. In these maps a projected contour plot is the floor and the 3-dimensional surface map resides directly above. The average value is given in the upper left-hand side of each plot. For the indents performed on the fully dense PTFE surface and the epoxy surface the average values of the hardness were $\langle H \rangle = 48$ MPa with standard

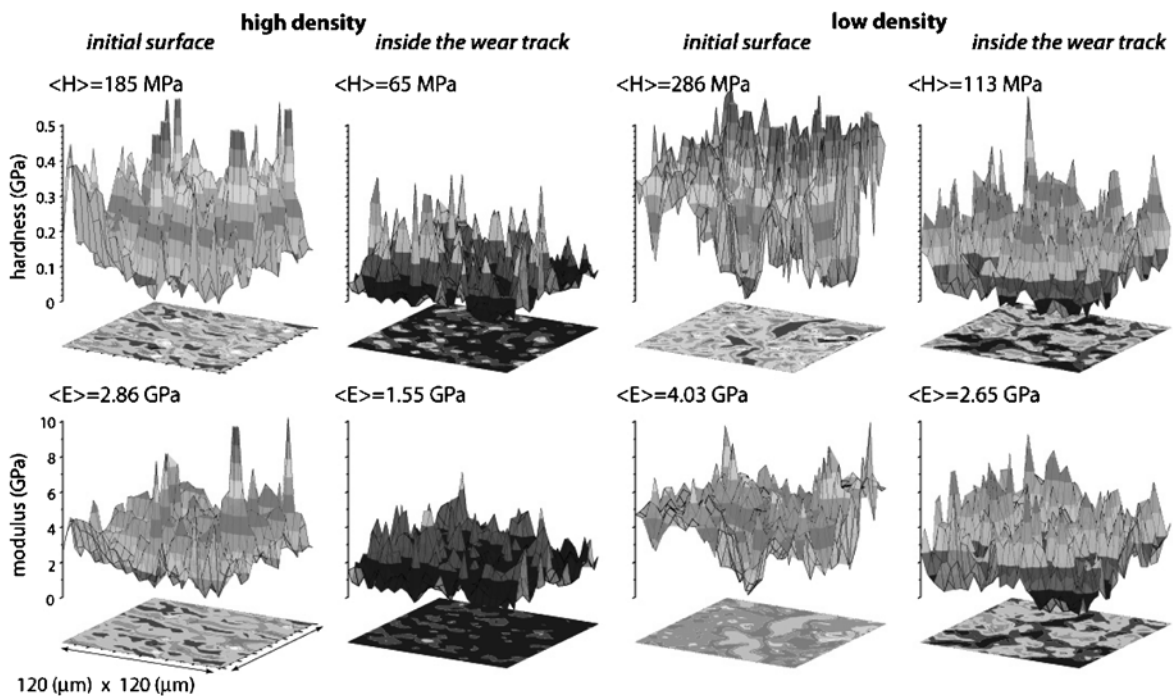


Figure 8. Nanoindentation of 625 indents placed uniformly over a 120 μm by 120 μm area on the initial unworn surfaces and a region inside the wear track were performed on films that were run under 2 N normal load and 1 m/s sliding speed. These are the same surfaces shown in figure 7.

deviation of $\sigma = 29$ MPa for the PTFE and $\langle H \rangle = 205$ MPa and $\sigma = 268$ MPa for the epoxy. The average values of the reduced modulus of elasticity were $\langle E \rangle = 1.32$ GPa with standard deviation of $\sigma = 0.55$ GPa for the PTFE and $\langle E \rangle = 4.64$ GPa and $\sigma = 2.68$ GPa for the epoxy.

The plot shown in figure 7 captures the compartmentalized nature of these original composites with the dark blue regions consistent with the hardness and modulus values of PTFE. The average elastic modulus of the original films was 2.86 and 4.03 GPa for the high density and low density composites respectively. Calculations of the composite elastic modulus using a linear rule-of-mixtures for the high density and low density composites are 2.76 and 3.47, respectively. This agreement between the expected values and the measured values is interesting considering the small size of the sampled region.

Inside the wear tracks both the hardness and modulus are reduced, suggesting increased PTFE concentration. Using the linear rule-of-mixtures to solve for the PTFE volume fraction in the wear track gives 0.93 and 0.60 for the high density and low density composites respectively. This nanomechanical testing supports the earlier hypothesis that the transfer films are PTFE rich. Further, the nodal shape, size, spacing, and volume fraction likely play key roles in whether or not the transfer films are either nearly pure PTFE overlaying the epoxy or a mixture of PTFE and epoxy.

5. Conclusion

This article reports on a new polymer composite coating that is comprised of PTFE nodes and fibrils encapsulated by epoxy. The friction coefficients were reduced over that of pure PTFE and the wear rates were reduced by over 100×. It is suggested that the mechanism for this reduction in both friction and wear is related to the PTFE being drawn out of the nodes and forming a transfer film over the epoxy regions.

Acknowledgments

A portion of this material is based upon work supported under NSF Grant No. #CMS-0219889, GO-

ALI: Collaborative Research: Tribology of Nanocomposites. Any opinions, findings, and conclusions or recommendations expressed in this material are those of the authors and do not necessarily reflect the views of the National Science Foundation.

References

- [1] J. Khedkar, I. Negulescu and E.I. Meletis, *Wear* 252 (2002) 361.
- [2] Y. Iwai, T. Honda, T. Onizuka, Y. Taniguchi and M. Kawabata, *J. Jpn. Soc. Tribol.* 45 (2000) 689.
- [3] F. Li, F.Y. Yan, L.G. Yu and W.M. Liu, *Wear* 237 (2000) 33.
- [4] Z.Z. Zhang, Q.J. Xue, W.M. Liu and W.C. Shen, *J. Appl. Poly. Sci.* 73 (1999) 2611.
- [5] Q.J. Xue, Z.Z. Zhang, W.M. Liu and W.C. Shen, *J. Appl. Poly. Sci.* 69 (1998) 1393.
- [6] J. Bijwe, S. Neje, J. Indumathi and M. Fahim, *J. Reinf. Plast. Comp.* 21 (2002) 1221.
- [7] F. Li, K.A. Hu, J.L. Li and B.Y. Zhao, *Wear* 249 (2001) 877.
- [8] W.G. Sawyer, K.D. Freudenberg, P. Bhimaraj and L.S. Schadler, *Wear* 254 (2003) 573.
- [9] J. E and D.T. Gawne, *Wear* 176 (1994) 195.
- [10] T. Tevruz, *Wear* 230 (1999) 61.
- [11] W.X. Chen, F. Li, G. Han, J.B. Xia, LY. Wang, J.P. Tu and Z.D. Xu, *Tribol. Lett.* 15 (2003) 275.
- [12] M. Kawamura, Y. Takeichi and M. Uemura, *J. Jpn. Soc. Tribol.* 48 (2003) 230.
- [13] X.H. Cheng, Y.J. Xue and C.Y. Xie, *Wear* 253 (2002) 869.
- [14] X.H. Cheng, Y.J. Xue, and C.Y. Xie, *Mater. Lett.* 57 (2003) 2553.
- [15] Z.Z. Zhang, Q.J. Xue, W.M. Liu and W.C. Shen, *Tribol. Int.* 31 (1998) 361.
- [16] B.R. Burroughs, J.H. Kim and T.A. Blanchet, *Tribol. Trans.* 42 (1999) 592.
- [17] S.E. Franklin and A. de Kraker, *Wear* 255 (2003) 766.
- [18] M. Kurokawa, Y. Uchiyama, T. Iwai and S. Nagai, *J. Tribol.-Trans. Asme* 125 (2003) 661.
- [19] O. Jacobs, R. Jaskulka, F. Yang and W. Wu, *Wear* 256 (2004) 9.
- [20] Q.H. Wang, Q.J. Xue, W.M. Liu and J.M. Chen, *Wear* 243 (2000) 140.
- [21] J.H. Jia, R.D. Zhou, S.Q. Gao and J.M. Chen, *Mater. Sci. Eng. A – Struct. Mater. Prop. Microstruct. Process.* 356 (2003) 48.
- [22] M.Q. Zhang, M.Z. Rong, S.L. Yu, B. Wetzel and K. Friedrich, *Wear*, 253 (2002) 1086.
- [23] G. Shi, M.Q. Zhang, M.Z. Rong, B. Wetzel and K. Friedrich, *Wear* in press.
- [24] G. Shi, M.Q. Zhang, M.Z. Rong, B. Wetzel and K. Friedrich, *Wear* 254 (2003) 784.
- [25] W. Brostow, P.E. Cassidy, H.E. Hagg, M. Jaklewicz and P.E. Montemartini, *Polymer* 42 (2001) 7971.
- [26] M.F. Doerner and W.D. Nix, *J. Mater. Res.* 1 (1986) 601.
- [27] W.C. Oliver and G.M. Pharr, *J. Mater. Res.* 7 (1992) 1564.